Macromolecules

Article

Cite This: Macromolecules 2019, 52, 9238−9247

pubs.acs.org/Macromolecules

Benzoic Acid as an Efficient Organocatalyst for the Statistical Ring-Opening Copolymerization of ε-Caprolactone and L-Lactide: A Computational Investigation

Coralie Jehanno,[†] Leila Mezzasalma,[‡,§] Haritz Sardon,[†] Fernando Ruipérez,[†] Olivier Coulembier,[*,‡] and Daniel Taton[*,§]

[†]POLYMAT, University of the Basque Country UPV/EHU, Joxe Mari Korta Center, Avda. Tolosa 72, 20018 Donostia-San Sebastián, Spain

[‡]Center of Innovation and Research in Materials and Polymers (CIRMAP), Laboratory of Polymeric and Composite Materials, University of Mons, 23 Place du Parc, Mons B-7000, Belgium

[§]Laboratoire de Chimie des Polymères Organiques (LCPO), CNRS, ENSCBP University of Bordeaux, UMR 5629, 16, av. Pey Berland 33607 Cedex, Pessac, France

Supporting Information

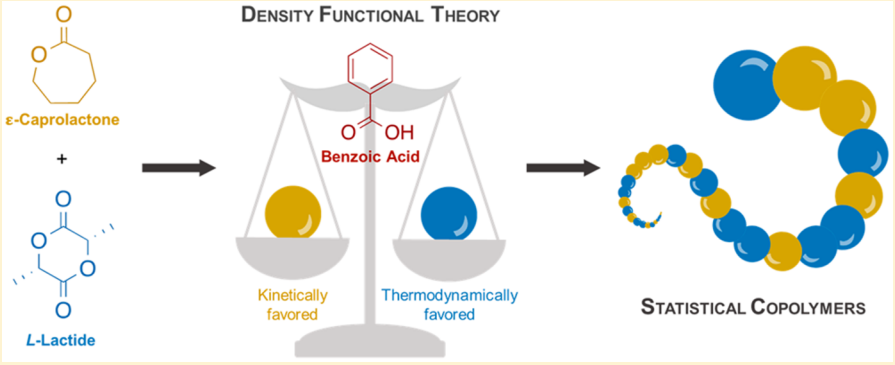

ABSTRACT: Statistical copolymers of L-lactide (L-LA) and ε-caprolactone (CL) are of major interest as a result of the desired combination of properties they exhibit for high-added-value applications, including in the biomedical field and in microelectronics. However, the high difference of reactivity between the two monomers makes difficult their statistical insertion in copolymer chains. Here, the ring-opening polymerization and copolymerization (ROP and ROcP, respectively) of L-LA and CL mediated by benzoic acid (BA) are investigated by means of density functional theory (DFT). It is first evidenced that the mechanism involves a hydrogen-bonding dual activation, where the acidic proton of BA activates the carbonyl moiety of the monomer, while the conjugated base of BA activates the alcohol initiator. In accordance with experimental findings, DFT calculations have then revealed a kinetically favored energetic profile for the BA-organocatalyzed ROP of CL compared to L-LA. In addition, energetic profiles of the BA-mediated ROcP of CL and L-LA does not show any preference of the insertion between CL and L-LA, irrespective of the type of growing species. Even though the caproyl unit insertion is kinetically favored by the primary nature of the growing chain end alcohol, this is eventually mitigated by the stabilizing effect of the ester moieties of the lactidyl unit, which is thermodynamically favored. As one effect compensates for the other, the dual activation mechanism involved in this organocatalytic pathway using BA as a weak organic acid is shown to be crucial to achieve truly statistical copolymers based on L-LA and CL.

INTRODUCTION

Poly(lactide) (PLA) and poly(ε-caprolactone) (PCL) are synthetic aliphatic polyesters widely investigated over the past decades for their biocompatibility and biodegradability. Yet, their respective ring-opening polymerization (ROP) leads to poor elasticity for PLA[1] and poor mechanical properties for PCL.[2] These antagonist properties make the statistical ring-opening copolymerization (ROcP) of lactide (LA) and ε-caprolactone (CL) a judicious choice for the synthesis of biodegradable materials with optimal thermomechanical properties. The resulting copolymers could for instance be used in pharmaceutical or biomedical applications.[3−5] However, control over the ROcP process is a key challenge because of a clearly distinct reactivity between the two monomers. Despite a significantly higher reactivity of CL over LA during their respective homopolymerizations, LA is

Received: September 4, 2019
Revised: October 30, 2019
Published: November 25, 2019

DOI: 10.1021/acs.macromol.9b01853
Macromolecules 2019, 52, 9238−9247

preferentially incorporated in the copolymer chain, especially for ROcP reactions catalyzed by organometallic complexes.[6] Up to now, only a few organometallic catalysts, especially aluminum-based salen complexes, have allowed achieving an actual controlled ROcP of LA and CL via the so-called coordination−insertion mechanism.[7−11] To get an insight into the key parameters influencing this reactivity differences, Chandanabodhi et al. have conducted density functional theory (DFT) calculations for both the ROP and the ROcP of the two monomers utilizing salen-type aluminum complexes.[12] LA has been found to exhibit a higher affinity toward the propagating species, which explains a lower kinetic rate in ROP (homopolymerization) reactions but, in the same time, a higher reactivity when both monomers are involved in ROcP (copolymerization).

Organocatalysts offer numerous advantages over their organometallic counterparts: they are more environmentally friendly, show a reduced toxicity and cost, and provide easier catalyst synthesis and storage. In addition, organocatalysts are often tolerant to functional groups; some remain active at elevated temperature, and a variety of solvents and even solvent-free conditions can be implemented, which facilitates advanced polymer design.[13−15] Their relative nontoxicity combined with their easy removal from the final polymer makes also organic catalysts suitable candidates for the design of materials intended for applications requiring biocompatibility.[16,17] Last but not least, organocatalysts often operate through different reaction mechanisms compared to organometallic catalysts,[13−15] for instance, through hydrogen-bonding activation, which might enable the specific synthesis of novel polymeric materials.[18−20]

The organocatalyzed ROP (OROP) of LA can be readily conducted in solution, typically in the presence of basic and/or nucleophilic catalytic compounds. The latter can operate either through an activated chain end mechanism (ACEM) or through a bifunctional activation pathway. However, conducting these reactions in bulk (solvent-free conditions) has met with very limited success.[21−23] As for Brønsted acid-type organocatalysts, they have been rarely applied for the same purpose, but trifluoromethanesulfonic acid and diphenyl phosphate have been successfully employed for the ROP of L-LA in solution and in bulk.[24−26] In contrast, acidic organocatalysts, such as sulfonic, phosphoric, boric, and carboxylic acids, have been largely and successfully employed for the ROP of CL in solution. Depending on the structure of the acid, ROP proceeds through the activated monomer mechanism (AMM) and/or through a bifunctional activation mechanism.[27−31]

Synthesis of statistical copolymers based on L-LA and CL, P(LA-*stat*-CL), remains very challenging, whatever the catalysts employed to this end.[28,32−36] This is due to the highly differing reactivity of the two monomers during ROcP. LA is typically incorporated first, although CL gives faster rates than LA in homopolymerization reactions. Recently, some of us have reported the ROP of L-LA and CL catalyzed by benzoic acid (BA) in bulk at 155 °C. Beyond the fact of being a cheap, thermally stable, and easily recyclable organocatalyst, BA has proven highly efficient to perform both the ROP and the ROcP of the two monomers. Remarkably indeed, both monomer units can be simultaneously inserted in the growing chain during ROcP, yielding truly statistical copolymers.[37,38]

Investigations into the individual ROP reaction mechanisms involving each of the two monomers and either organometallic[39−43] or organic catalysts,[44−50] have been reported. In this context, the study by Chandanabodhi et al. regarding the relative reactivity of the monomers in ROcP remains an exception.[12] Yet, correlating the reaction rates with the catalyst's structure appears essential to understand the cause of the unexpected random character of copolymers resulting from the BA-organocatalyzed ROcP of L-LA and CL. It thus appears that a more detailed investigation is needed to gain a deeper insight into elementary reactions possibly involved in the RO(c)P process. For this purpose, we have used theoretical methods of quantum chemistry, namely, DFT, to model experimental findings regarding both the ROP and the ROcP of L-LA and CL employing BA as an organic catalyst. We thus provide here a comprehensive vision of the reaction mechanism operating during the synthesis of PLA, PCL, and P(LA-*stat*-CL) copolymers when employing a weak acidic-type organocatalyst such as BA. Not only these calculations support our experimental findings, but they also reveal the specificity of this organocatalytic pathway to achieve statistical copolymers based on L-LA and CL.

RESULTS AND DISCUSSION

Computational Details. All calculations were performed with the Gaussian 16 suite of programs.[51] Geometry optimizations were performed in solution, using the ωB97X-D functional[52] and the 6-31+G(d,p) basis set of double-ζ quality plus diffuse and polarization functions, at T = 428 K. This functional is particularly well suited to describe weak interactions, such as hydrogen bonds. Solvent effects were estimated by using the polarizable continuum model (PCM) approach,[53−56] with the dielectric constant of caprolactone (CL) at room temperature (ε^{CL} = 36.5). To confirm that the optimized structures were minima on the potential energy surfaces, frequency calculations were performed at the same level of theory and then used to evaluate the zero-point vibrational energy (ZPVE) and the thermal vibrational corrections. The transition states are characterized by a single imaginary frequency corresponding to the displacement in the reaction coordinate that connects reactants and products. The electronic energy was refined by single-point energy calculations at the ωB97X-D/6-311++G(2df,2p) level of theory, using a triple-ζ basis set plus polarization and diffuse functions.

Investigation into the ROP Reaction Mechanism. Based on the background literature, three distinct reaction mechanisms can be envisaged regarding the use of BA as a weak Brønsted acid-type organocatalyst for both the ROP and ROcP of L-LA and CL. In the AMM, the acid protonates the carbonyl group of the monomer to facilitate the nucleophilic attack of the initiator (or propagating chain), which is followed by ring opening (Scheme S1, path I). In the dual (bifunctional) activation mechanism, while the acidic moiety of the catalyst interacts with the carbonyl of the monomer by protonation, the basic moiety activates the hydroxyl group of the initiator (and, then, of propagating chain ends) (Scheme S1, path II). Contrary to these two hydrogen-bond-based mechanisms, a third reaction pathway involving the dual activation of the catalyst through acetyl transfer has also been reported for another well-known organocatalyst, the triazabicyclodecene (TBD).[44,46] The Hedrick group has indeed suggested a pathway involving a preliminary opening of the monomer through catalyst insertion by protonation of the oxygen atom of the cyclic ester. This is followed by the nucleophilic attack of the initiator/propagating chain activated by the deprotonated

DOI: 10.1021/acs.macromol.9b01853
Macromolecules 2019, 52, 9238−9247

catalyst (Scheme S1, path III). These three plausible mechanisms were thus investigated by DFT calculations, for the BA-OROP of both CL and L-LA, using ethanol as initiator. The search of transition states (TS) for the three mechanisms led to the isolation of an optimized structure only for path II and path III (**TS1-II** and **TS1-III**). Computations related to the AMM (path I) indeed resulted in the same transition state (**TS1-II**) to that pertaining to the hydrogen-bond-based dual activation mechanism (path II). Therefore, this mechanism was not explored further and only the energetic profiles of path II and path III were compared for L-LA (Figure 1a) and CL (Figure 1b).

The energetic barriers for **TS1-III** reached 31.4 and 33.7 kcal mol^{-1} for L-LA and CL, respectively, while the energy required for overcoming **TS1-II** was found equal to 16.1 and 15.7 kcal mol^{-1} only. The first transition state being rate-determining for path II (Figures S1 and S2), these numbers clearly demonstrated that the dual activation pathway (path II) is energetically favored for both monomers compared to the covalently bound pathway (path III). In such a way, a concomitant activation of the carbonyl of the lactone and the hydroxyl of the initiator can be proposed. These findings are very consistent with the mechanistic studies previously reported for ROP of cyclic esters or cyclic carbonates employing much stronger acid organocatalysts, such as sulfonic acid and phosphoric acid.[45,48,49]

HOMOPOLYMERIZATION (ROP) STUDIES

Both the initiation and the propagation of the ROP of L-LA and CL were then investigated and compared by means of DFT calculations (Scheme 1). Initiation involves the opening of the cyclic ester to yield the *opened*-L-LA or the *opened*-CL, corresponding to the initial propagating chain of the polymer. The propagation step then implies the opening of a second monomer substrate by a nucleophilic attack of the linear opened species, yielding a propagating chain composed of two monomeric units, *prop*-LLA-LLA and *prop*-CL-CL. Both steps the initiation (**I**) and the propagation (**P**) proved to involve two TS. These included (1) the nucleophilic attack of the hydroxyl function of the initiator or the propagating chain on the lactone (**TS1**) and (2) the ring-opening of the cyclic monomer (**TS2**).

As for the ROP of L-LA, two nucleophilic attacks can be envisaged, i.e., on the nonsubstituted side (attack 1) or on the methyl-substituted side of L-LA (attack 2). As no significant difference was observed between the energetic barriers of both attacks, the reaction pathway involving attack 2 was therefore considered for a comparison between CL and L-LA (Figure S3).

Calculations revealed that the initiation step did not show any significant energetic differences. **TS1 I** indeed proved to be the rate-determining step for both L-LA and CL, 15.7 and 16.1 kcal mol^{-1} vs 11.0 and 11.8 kcal mol^{-1} for **TS2 I**, respectively (Figure 2). Although the optimized structures for the first transition state (**TS1 I**) demonstrated a better affinity between the carbonyl of CL and the catalyst, relative to L-LA, it did not seem to affect the energetic barrier (Figure S4). In particular, the optimized structure of **TS1 I** evidenced a complete deprotonation of the acidic moiety of BA for the ROP of CL, with a distance of 1.03 Å between this proton and the oxygen atom of the carbonyl group, while that between the proton and the oxygen atom of BA was extended to 1.47 Å. Conversely, for **TS1 I** involved in the ROP of L-LA, the acidic proton remained closer to the catalyst—a distance of 1.21 Å from the oxygen atom of the carbonyl group and only 1.18 Å from the oxygen atom of BA. This result is in accordance with experimental results found by ^{13}C NMR spectroscopy; a higher shift was observed for the interaction involving BA and

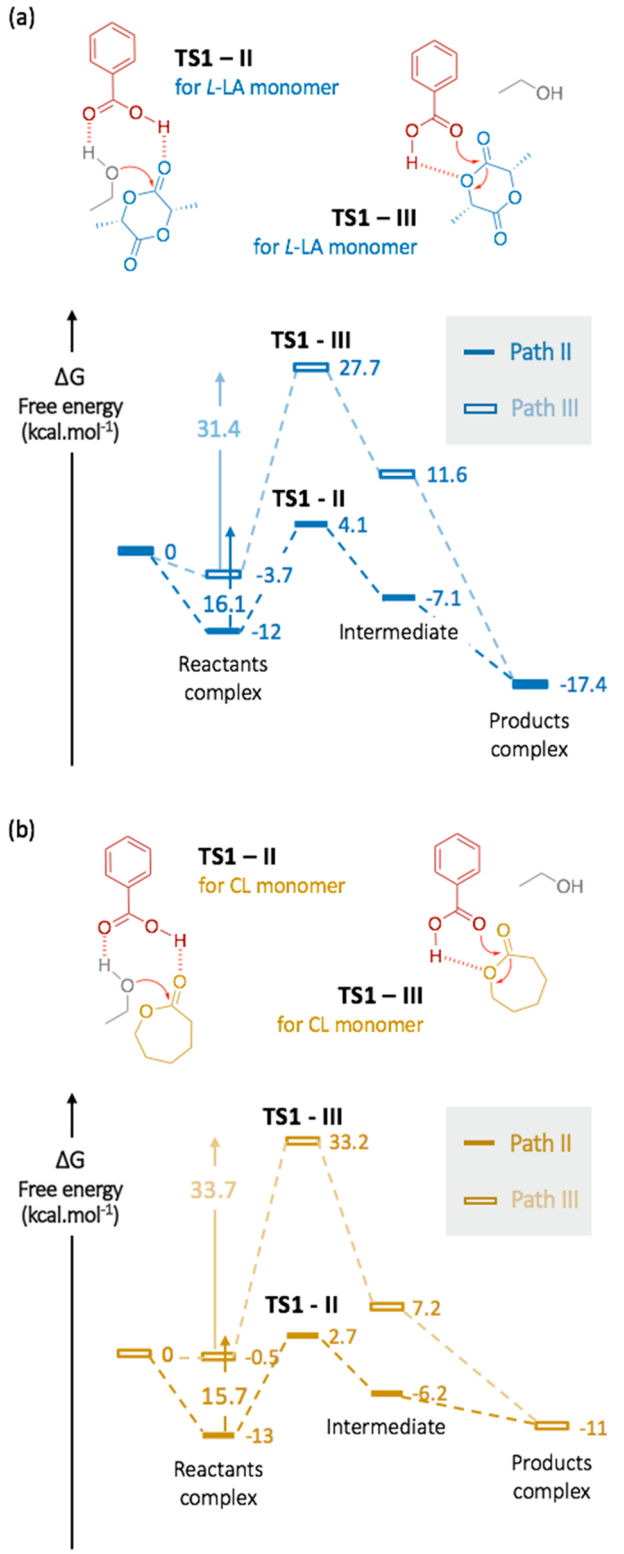

Figure 1. Comparison between the H-bonding (path II) and the acetyl transfer (path III) dual activation for **TS1** of the homopolymerization of (a) L-LA and (b) CL.

DOI: 10.1021/acs.macromol.9b01853
Macromolecules 2019, 52, 9238−9247

Scheme 1. Model Reactions for the ROP of (a) L-LA and (b) CL

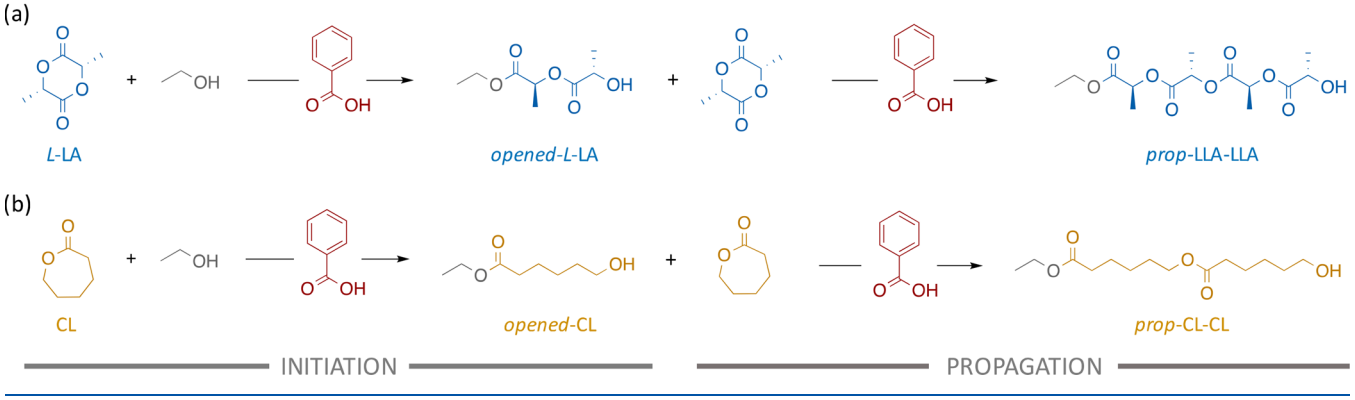

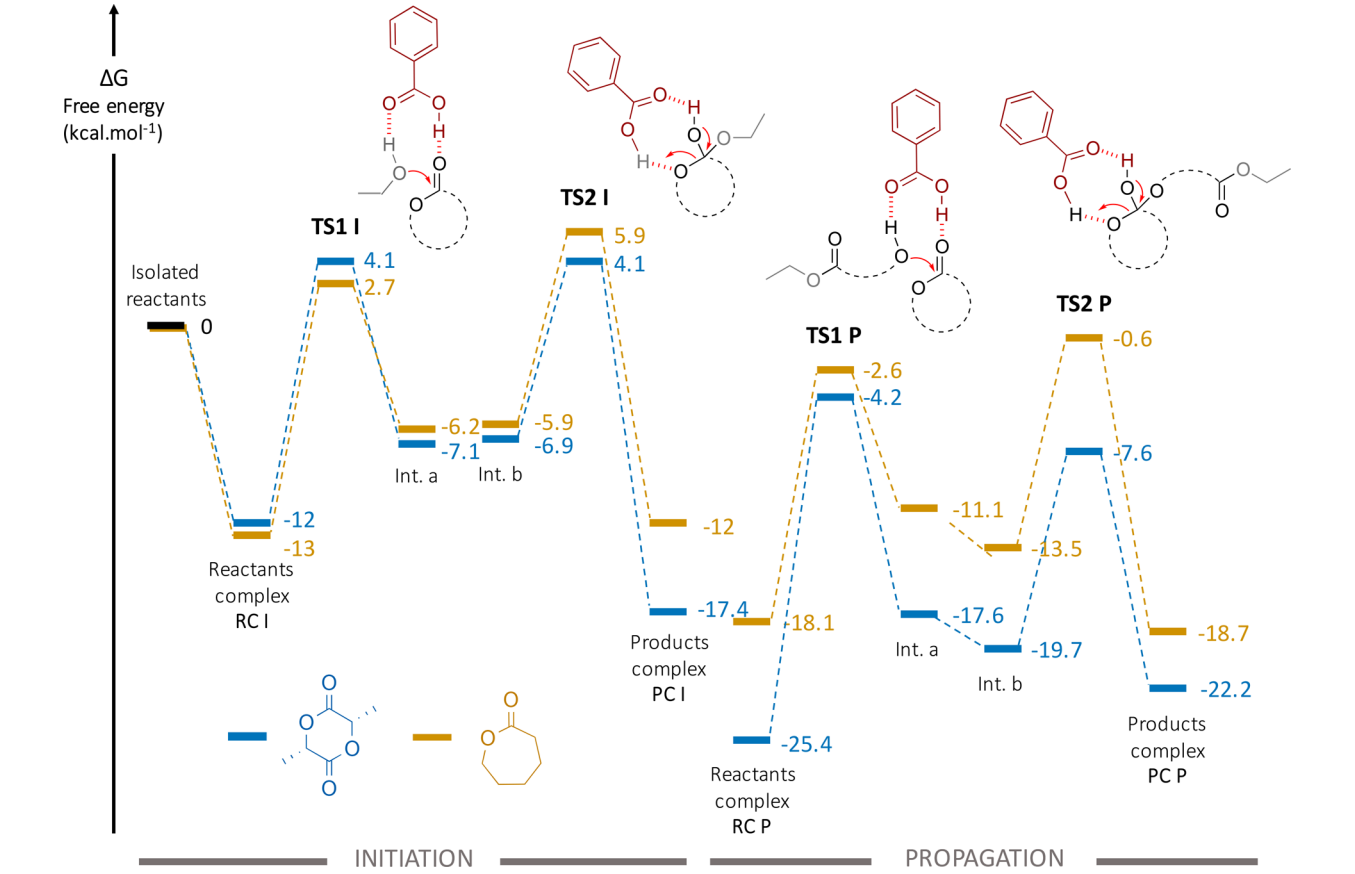

Figure 2. Energetic profile for the initiation and the propagation of the ROP of L-LA (blue) and CL (yellow) catalyzed by BA.

the carbonyl group of CL, suggesting a greater activation of this monomer.[38] Only a variation of the energetic profiles for the initiation step was noted for the final product complex, **PC I**, consisting of an *open*-CL or an *open*-L-LA unit in interaction with the catalyst and which was found significantly more stable for L-LA (−17.4 kcal mol^{-1}) than for CL (−12 kcal mol^{-1}). This *open*-CL unit seemed to adopt a constrained conformation because of the long alkyl chain of the caproyl unit between the terminal hydroxyl and the ester moiety (**PC I** for CL). As for the optimized structure for the *opened*-L-LA unit, it was found in interaction with the catalyst, forming a nine-member ring between BA and the ester moiety of the lactidyl unit (**PC I** for L-LA, Figure 3a).

Similar to **PC I**, the initial complex of the propagation step, **RC P**, which involves the catalyst, the propagating chain (*opened*-CL or *opened*-L-LA), and a new monomer molecule, was found lower in energy for L-LA, i.e., −25.4 and −18.1 kcal mol^{-1} for L-LA and CL, respectively. This again demonstrates the higher stability of complexes involving L-LA and BA relative to CL. However, and contrary to the initiation step, the energetic barriers involved in the rate-determining propagation step for (**TS1 P**) appeared to be different for the two monomers. While 21.2 kcal mol^{-1} was required to overcome **TS1 P** for L-LA, only 15.5 kcal mol^{-1} was needed for CL (Figure 2). This difference in energy may be explained by the different nature of the propagating alcohol. ROP of CL indeed involves primary alcohols, while ROP of L-LA generates secondary alcohols that are more sterically hindered. Thus, the nucleophilic attack for the ROP of L-LA may be impeded by steric hindrance of the methyl group in the α-position of the

DOI: 10.1021/acs.macromol.9b01853
Macromolecules 2019, 52, 9238−9247

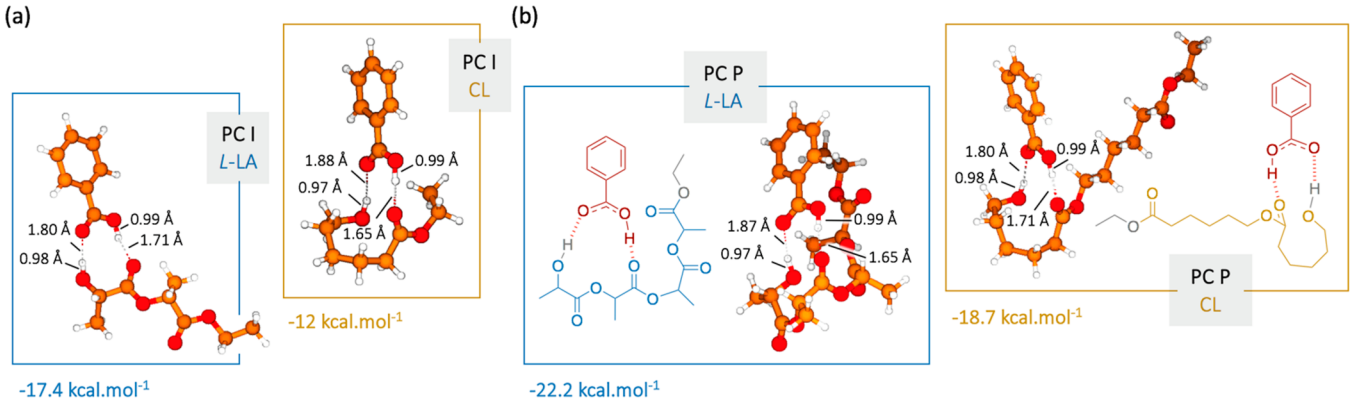

Figure 3. Optimized structures for the products complexes of (a) the initiation (**PC I**) and (b) the propagation (**PC P**) for L-LA (blue) and CL (yellow).

carbonyl of the monomer (Figures S3 and S4). These theoretical results thus confirm experimental findings, as the BA-catalyzed ROP of L-LA proved much slower (40 h) than that of CL (2 h) under otherwise identical conditions.[38]

Additionally, for the ROP of CL, it can be noticed that the energetic barriers for both **TS1** and **TS2** are very similar for the propagation and the initiation steps (**TS1 I** ≈ **TS1 P** and **TS2 I** ≈ **TS2 P**). This indicates that the rate of initiation is not higher than that of propagation, i.e., $k_i \approx k_p$, with k_i and k_p being the rate constants of initiation and propagation, respectively. Experimentally, an induction period before a linear evolution of $\ln([M]_0/[M])$ vs time was observed, which was ascribed to a slow initiation for the ROP of CL. In contrast, the ROP of L-LA is characterized by a greater energetic barrier for the propagation step (**TS1 P** = 21.2 kcal mol^{-1} and **TS1 I** = 16.1 kcal mol^{-1}), suggesting that $k_p < k_i$. These results are also in accordance with the pseudo-first-order kinetic plot found experimentally.[38]

Similar to **PC I** at the end of the initiation step, **PC P** proved to be lower in energy for the ROP of L-LA than for the ROP of CL, −22.2 kcal mol^{-1} vs −18.7 kcal mol^{-1}, respectively. The complex involving the *prop*-LLA-LLA unit stabilized by BA was found more stable because of the different ester moieties enabling a less constrained conformation for the propagating chain (Figure 3b). The particular coiled conformation adopted by *prop*-LLA-LLA after ring-opening likely favored hydrogen-bonding between ester moieties of the two lactidyl units and BA. In contrast, the rigidity of the long alkene chain observed for *prop*-CL-CL growing species exhibited an extended conformation, resulting in a less stable complex.

In the specific case of the ROP of L-LA, the bifunctional activation pathway by BA might also lead to a side reaction, namely, epimerization (Figure 4a). BA might form *meso*-lactide (*meso*-LA) by simultaneous protonation of L-LA and deprotonation of the α-methine (CH) group (**TS1 Ep**). The resulting planar enol that is stabilized by a mesomeric effect can undergo the exact opposite reaction on the other side of the lactone, with BA protonating back the α-position before deprotonating the carbonyl to get *meso*-LA (**TS2 Ep**). The energy required for overpassing both TSs involved in the epimerization of L-LA was found very similar, i.e., 26.1 and 27.4 kcal mol^{-1} for **TS1 Ep** and **TS2 Ep**, respectively (Figure 4b). This energetic barrier is higher than that calculated for **TS1 P** (≈ 21.2 kcal mol^{-1}) but is close enough so that this side reaction cannot be neglected, especially at such a high temperature (155 °C).

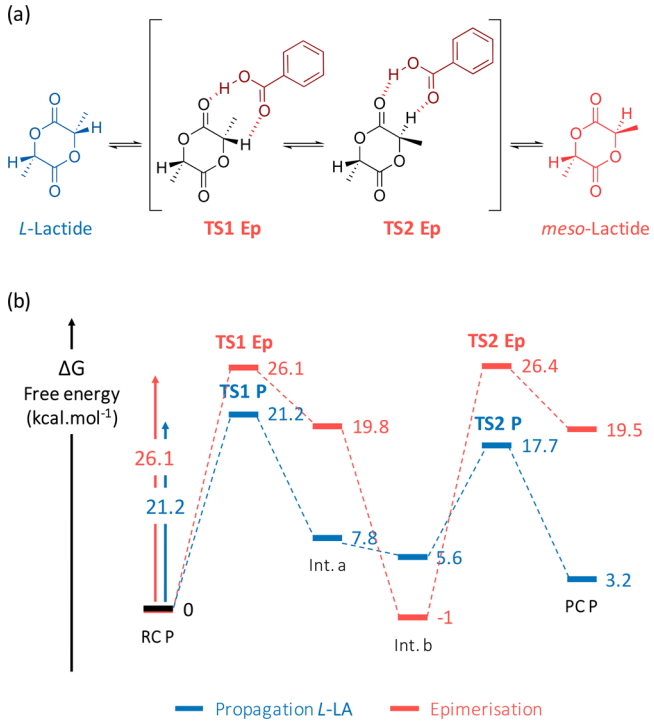

Figure 4. (a) Epimerization side-reaction for L-LA catalyzed by BA and (b) the comparative energetic profiles for the epimerization and the ROP propagation of L-LA.

From an experimental viewpoint, the butanediol-initiated BA-OROP of L-LA performed at 155 °C in bulk revealed the presence of signals characteristic of *meso*-LA by ^{1}H NMR spectroscopy. Model experiments performed at the polymerization temperature with only the monomer or only the initiator confirmed that the catalyst favored the formation of *meso*-LA, going from 3% of *meso*-LA with the sole L-LA to 8% with butanediol and 17% with BA (Figures S5−S8). The energetic profile discussed here is thus in accordance with experimental data.[38]

Copolymerization (ROcP) Studies. For the ROcP of L-LA and CL, two different propagation pathways can be envisaged, namely, from the caproyl and from the lactidyl chain end. These sequences refer to as *prop*-CL-CL and *prop*-CL-LLA, when initiated by an *open*-CL unit, and *prop*-LLA-LLA and *prop*-LLA-CL when initiated by an *open*-L-LA unit. The first term thus refers to the terminal unit of the growing chain,

DOI: 10.1021/acs.macromol.9b01853
Macromolecules 2019, 52, 9238−9247

whereas the second term corresponds to the last inserted monomer unit. Model reactions employed for the ROcP study follow the same pathway to that discussed for ROP reactions (Figures 5a and 6a), and calculations were conducted using the same conditions.

When the chain end is a caproyl unit, the subsequent addition of L-LA or CL did not show any energetic differences (Figure 5b). Indeed, the energetic barriers for **TS1 P** and **TS2 P**, as well as the energetic levels of the starting and ending complexes (**RC P** and **PC P**), were found almost the same, suggesting that both units could be indifferently inserted. The comparison of the optimized structures for **TS1 P** and **TS2 P** demonstrated similar conformations at the catalytic site,

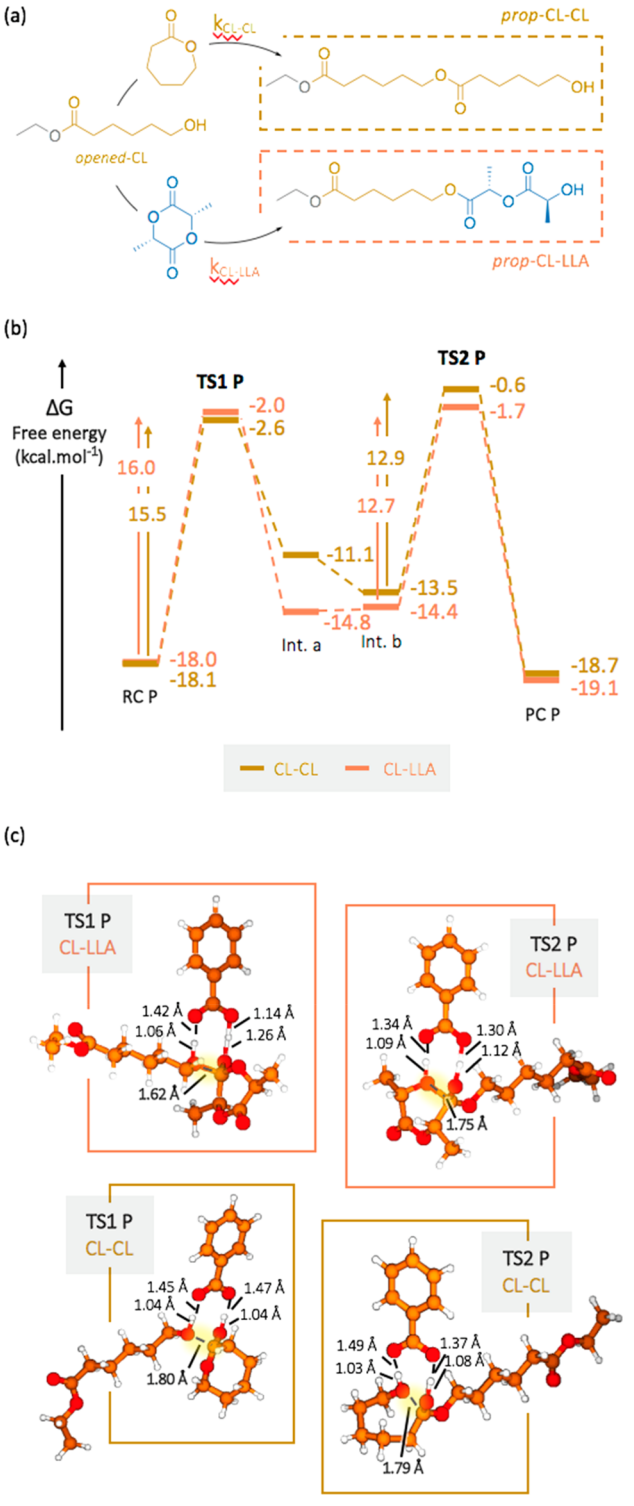

Figure 5. (a) Model reactions for the copolymerization of L-LA and CL initiated by a caproyl unit with (b) the related energetic profile and (c) optimized structures for **TS1 P** and **TS2 P**.

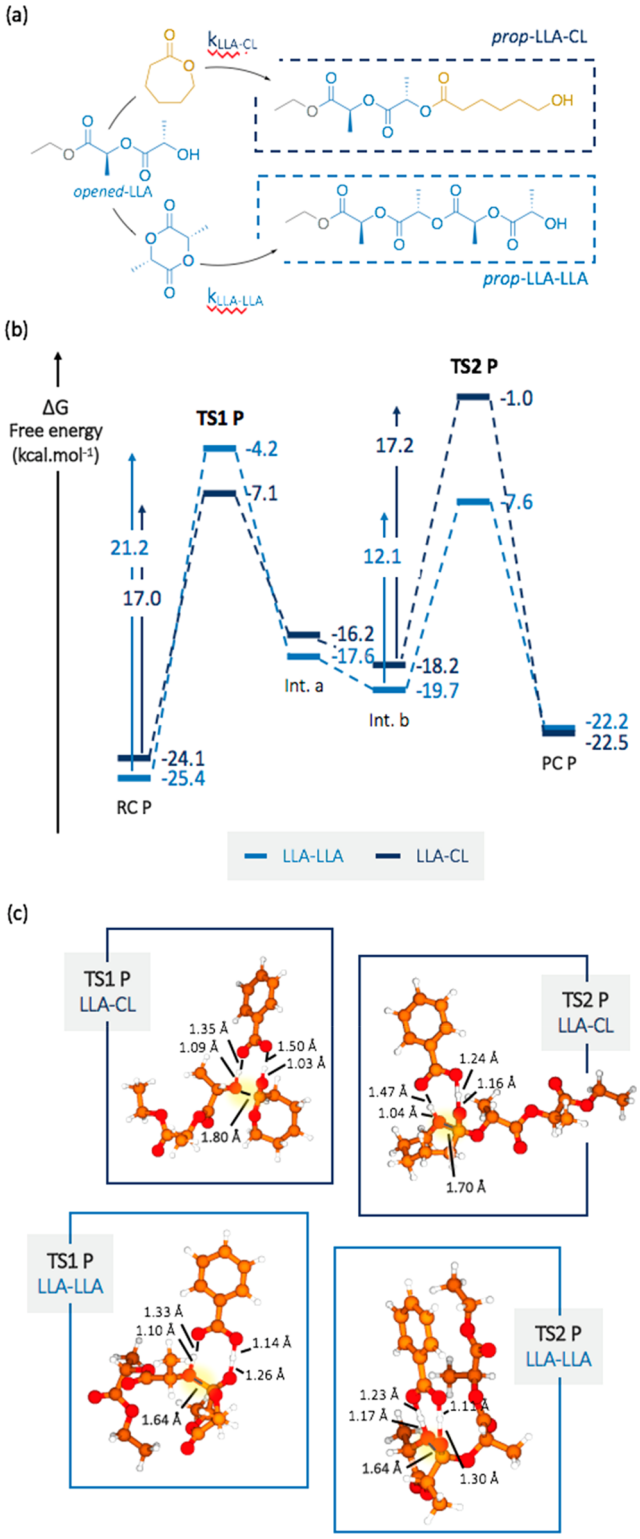

Figure 6. (a) Model reactions for the copolymerization of L-LA and CL initiated by a lactidyl unit with (b) the related energetic diagram with (c) optimized for **TS1 P** and **TS2 P**.

DOI: 10.1021/acs.macromol.9b01853
Macromolecules 2019, 52, 9238−9247

irrespectively of the nature of the added monomer (Figure 5c). Indeed, the alkene chain of the penultimate caproyl unit remained distant from the catalytic site, avoiding any interaction with BA and keeping an angle close to 90° between the planar catalyst and the caproyl tail. Additionally, and similarly to observations made for the initiation step, the distances between the acidic proton of BA and both the acidic oxygen of BA and the carbonyl oxygen of the monomer supported not only the occurrence of a complete deprotonation of the acid but also the fact that CL was preferentially incorporated, d(C═O−H) = 1.04 Å, if compared to L-LA monomer, d(C═O−H) = 1.26 Å.

In contrast, differences were noted between the two reaction pathways involving the lactidyl chain end (Figure 6b). Considering **TS1 P**, the attack on CL is kinetically favored by 4.2 kcal mol^{-1} over the attack on L-LA, 17 kcal mol^{-1} for *prop*-LLA-CL vs 21.2 kcal mol^{-1} for *prop*-LLA-LLA. Propagation involving a LLA-LLA dyad showed that the lactidyl tail could interact with L-LA to adopt a coiled conformation because of the methyl in the α-position of both the lactidyl penultimate unit and L-LA (Figure 6c). In contrast, propagation via a LLA-CL dyad revealed that ester moieties of the lactidyl unit adopted a free conformation, which did not interfere with the catalytic site, providing a lower energy to overcome the first TS. However, if **TS1 P** appeared to be the rate-determining step for the formation of *prop*-LLA-LLA (21.2 kcal mol^{-1} for **TS1 P** and 12.1 kcal mol^{-1} for **TS2 P**), the same was not true for propagation involving a *prop*-LLA-CL dyad. Both energetic barriers proved indeed to be very close (17 and 17.2 kcal mol^{-1}), supporting that this pathway was not only controlled by **TS1 P** but also that the energetic barrier required for **TS2 P** should be taken into account. Similar to observations made for TS involving a caproyl tail (Figure 5c), the lactidyl penultimate unit seemed to retain an extended conformation, remaining distant from BA, the rigidity of the last CL unit inserted likely hindering a more stable conformation (Figure 6c). Oppositely, for LLA-LLA propagation, the coiled conformation adopted by the lactidyl tail and the related weak interactions with the catalyst likely contributed to the stabilization of **TS2 P** in this case.

Thus, the more favored pathway for one TS being the less favored for the other, both effects are probably compensating each other, so that both pathways are plausible. A possible explanation for these opposite effects again relates to the flexibility of the lactidyl chain end and the rigidity of the alkene chain of CL. The nucleophilic attack of the propagating chain end on the cyclic monomer (**TS1 P**) requires more energy for the formation of *prop*-LLA-LLA because of the higher steric hindrance notably caused by the methyl in the α-position of the carbonyl for both the lactidyl chain end and L-LA. After ring-opening of the monomer (**TS2 P**), however, the flexibility of the lactidyl units seems to stabilize the transition state compared to the rigid alkyl chain of CL forming the *prop*-LLA-CL chain end.

Experimentally, even though the ROP of CL provided faster reaction relative to the ROP of L-LA, both monomers could be evenly inserted in the copolymer chain, giving rise to statistical copolymers. Reactivity ratios of both monomers were found equal to 0.86, supporting a random insertion, whether chain ends were of caproyl (r_{CL}) or lactidyl type (r_{LLA}).[57]

$$r_{CL} = \frac{k_{CL\text{-}CL}}{k_{CL\text{-}LLA}} \quad \text{and} \quad r_{LLA} = \frac{k_{LLA\text{-}LLA}}{k_{LLA\text{-}CL}} \qquad (1)$$

Notably, by comparing the energy of **PC P** for the four different pathways, it can be noticed that the energetic levels of *prop*-LLA-LLA and *prop*-LLA-CL are more stable of around 3−4 kcal mol^{-1} than *prop*-CL-CL and *prop*-CL−LLA (Figures 5b and 6b). This means that the penultimate unit has a greater effect on the stabilization of the copolymer, as while it is a lactidyl, the complex resulting from the ring-opening is lower in energy. Optimized structures of **PC P** for propagating CL-LLA and LLA-CL reveal favorable interactions between the ester moieties of the lactidyl unit and the catalyst compared to the caproyl unit (Figure 7). This can be correlated to the

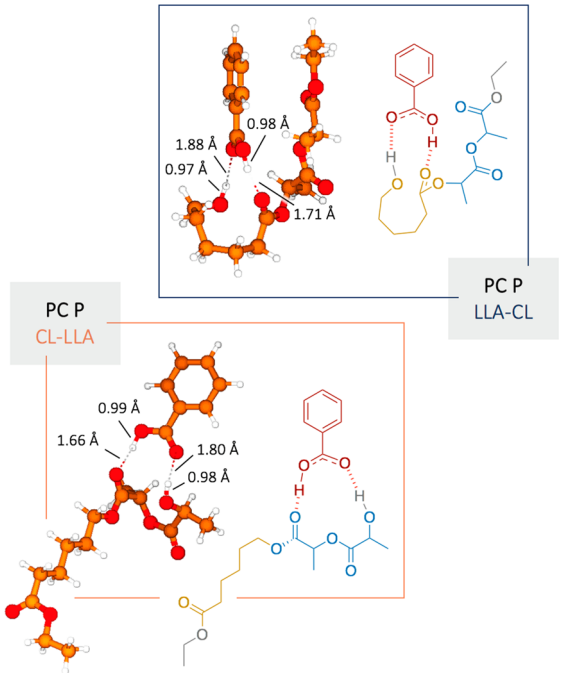

Figure 7. Schemes and optimized structures for the propagation products complexes (**PC P**) for (a) the addition of a ε-caprolactone on a lactidyl unit (LLA-CL) and (b) the addition of a lactide unit on a caproyl unit (CL-LLA).

stabilization effect observed for the propagation via the LLA-CL dyad relatively to that involving a CL-LLA dyad. Finally, and very importantly, the energetic barriers involved in these four reaction pathways remain close in energy, suggesting that all of them appear to be plausible. All TS, intermediates, and complexes involved in the propagation step are lower in energy than those of the initiation step, meaning that the propagation is exergonic, a typical pattern for active ROP reactions (Figures S9 and S10).[46]

CONCLUSION

Density functional theory (DFT) calculations have shown that benzoic acid (BA) proceeds via a bifunctional activation mechanism to catalyze the ring-opening polymerization (ROP) of L-lactide (L-LA) and ε-caprolactone (CL). Computational results support experimental findings for both homopolymerizations of L-LA and CL. The ROP of L-LA is characterized by a slower reaction rate compared to the ROP of CL because of both the steric hindrance of the methyl group at the propagating chain end and the methyl group in the α-position of L-LA. Besides, DFT calculations have evidenced that epimerization transforming L-LA into *meso*-LA is highly likely

DOI: 10.1021/acs.macromol.9b01853
Macromolecules 2019, 52, 9238−9247

during the BA-organocatalyzed ROP of L-LA. Finally, investigations by DFT of ring-opening copolymerization (ROcP) experiments revealed that caproyl unit insertion is kinetically favored, providing lower energetic barriers because of a chain growth by a primary alcohol at the chain end alcohol, while insertion of lactidyl units is thermodynamically favored, providing lower energetic levels because of the stabilizing effect of the corresponding ester moieties. These opposite effects enable the use of BA as a weak organic acid for the precise synthesis of true statistical copolymers based on L-LA and CL. We expect that BA could be applied to ROcP of other heterocyclic monomers for the design of new copolymer structures.

■ ASSOCIATED CONTENT

Supporting Information

The Supporting Information is available free of charge at https://pubs.acs.org/doi/10.1021/acs.macromol.9b01853.

Energetic profile of the two different attacks for the ROP of L-LA; optimized structures for the reactant complexes with detailed distances; energetic profiles for the homopolymerization of L-LA and CL with optimized structures; ^{1}H NMR study for the epimerization of L-LA; energetic profiles for the copolymerization of L-LA and CL (PDF)

■ AUTHOR INFORMATION

Corresponding Authors

*(D.T.) E-mail taton@enscbp.fr.

*(O.C.) E-mail olivier.coulembier@umons.ac.be.

ORCID

Coralie Jehanno: 0000-0003-3180-2834

Haritz Sardon: 0000-0002-6268-0916

Fernando Ruipérez: 0000-0002-5585-245X

Olivier Coulembier: 0000-0001-5753-7851

Daniel Taton: 0000-0002-8539-4963

Author Contributions

C.J. and L.M. contributed equally to this work.

Notes

The authors declare no competing financial interest.

■ ACKNOWLEDGMENTS

This work was supported by the EU Horizon 2020 Research and Innovation Framework Program—European Joint Doctorate—SUSPOL-EJD (grant 642671), by the European Commission and Region Wallonne FEDER program and OPTI2MAT program of excellence, by the Interuniversity Attraction Pole Programme (P7/05) initiated by the Belgian Science office, and by the FNRS-FRFC. Technical and human support provided by IZO-SGI, SGIKer (UPV/EHU, MICINN, GV/EJ, ERDF, and ESF) is gratefully acknowledged for assistance and generous allocation of computational resources. O.C. is Research Associate for the F.R.S.-FNRS in Belgium.

■ ABBREVIATIONS

PLA, poly(lactide); PCL, poly(ε-caprolactone); ROP, ring-opening polymerization; ROcP, ring-opening copolymerization; LA, lactide; CL, ε-caprolactone; DFT, density functional theory; OROP, organocatalyzed ring-opening polymerization; ACEM, activated chain end mechanism; AMM, activated monomer mechanism; BA, benzoic acid; PCM, polarizable continuum model; ZPVE, zero-point vibrational energy; TS, transition state.

■ REFERENCES

(1) Martin, O.; Avérous, L. Poly(Lactic Acid): Plasticization and Properties of Biodegradable Multiphase Systems. *Polymer* **2001**, *42* (14), 6209−6219.

(2) Sisson, A. L.; Ekinci, D.; Lendlein, A. The Contemporary Role of ε-Caprolactone Chemistry to Create Advanced Polymer Architectures. *Polymer* **2013**, *54* (17), 4333−4350.

(3) Jung, Y.; Park, M. S.; Lee, J. W.; Kim, Y. H.; Kim, S.-H.; Kim, S. H. Cartilage Regeneration with Highly-Elastic Three-Dimensional Scaffolds Prepared from Biodegradable Poly(L-Lactide-Co-ε-Caprolactone). *Biomaterials* **2008**, *29* (35), 4630−4636.

(4) Cha, K. J.; Lih, E.; Choi, J.; Joung, Y. K.; Ahn, D. J.; Han, D. K. Shape-Memory Effect by Specific Biodegradable Polymer Blending for Biomedical Applications: Shape-Memory Effect by Specific Biodegradable Polymer. *Macromol. Biosci.* **2014**, *14* (5), 667−678.

(5) Kim, S. H.; Kim, S. H.; Jung, Y. TGF-β 3 Encapsulated PLCL Scaffold by a Supercritical CO_2 − HFIP Co-Solvent System for Cartilage Tissue Engineering. *J. Controlled Release* **2015**, *206*, 101−107.

(6) Stirling, E.; Champouret, Y.; Visseaux, M. Catalytic Metal-Based Systems for Controlled Statistical Copolymerisation of Lactide with a Lactone. *Polym. Chem.* **2018**, *9* (19), 2517−2531.

(7) Nomura, N.; Akita, A.; Ishii, R.; Mizuno, M. Random Copolymerization of ε-Caprolactone with Lactide Using a Homosalen-Al Complex. *J. Am. Chem. Soc.* **2010**, *132* (6), 1750−1751.

(8) Wang, Y.; Ma, H. Exploitation of Dinuclear Salan Aluminum Complexes for Versatile Copolymerization of ε-Caprolactone and L-Lactide. *Chem. Commun.* **2012**, *48* (53), 6729−6731.

(9) Shi, T.; Luo, W.; Liu, S.; Li, Z. Controlled Random Copolymerization of Rac-Lactide and ε-Caprolactone by Well-Designed Phenoxyimine Al Complexes. *J. Polym. Sci., Part A: Polym. Chem.* **2018**, *56* (6), 611−617.

(10) Honrado, M.; Otero, A.; Fernández-Baeza, J.; Sánchez-Barba, L. F.; Garcés, A.; Lara-Sánchez, A.; Rodríguez, A. M. Copolymerization of Cyclic Esters Controlled by Chiral NNO-Scorpionate Zinc Initiators. *Organometallics* **2016**, *35* (2), 189−197.

(11) Maruta, Y.; Abiko, A. Random Copolymerization of ε-Caprolactone and L-Lactide with Molybdenum Complexes. *Polym. Bull.* **2014**, *71* (4), 989−999.

(12) Chandanabodhi, D.; Nanok, T. A DFT Study of the Ring-Opening Polymerization Mechanism of l -Lactide and ε -Caprolactone Using Aluminium Salen-Type Initiators: Towards an Understanding of Their Reactivities in Homo- and Copolymerization. *Mol. Catal.* **2017**, *436*, 145−156.

(13) Kiesewetter, M. K.; Shin, E. J.; Hedrick, J. L.; Waymouth, R. M. Organocatalysis: Opportunities and Challenges for Polymer Synthesis. *Macromolecules* **2010**, *43* (5), 2093−2107.

(14) Dove, A. P. Organic Catalysis for Ring-Opening Polymerization. *ACS Macro Lett.* **2012**, *1* (12), 1409−1412.

(15) Ottou, W. N.; Sardon, H.; Mecerreyes, D.; Vignolle, J.; Taton, D. Update and Challenges in Organo-Mediated Polymerization Reactions. *Prog. Polym. Sci.* **2016**, *56*, 64−115.

(16) Nachtergael, A.; Coulembier, O.; Dubois, P.; Helvenstein, M.; Duez, P.; Blankert, B.; Mespouille, L. Organocatalysis Paradigm Revisited: Are Metal-Free Catalysts Really Harmless? *Biomacromolecules* **2015**, *16* (2), 507−514.

(17) Xia, Y.; Shen, J.; Alamri, H.; Hadjichristidis, N.; Zhao, J.; Wang, Y.; Zhang, G. Revealing the Cytotoxicity of Residues of Phosphazene Catalysts Used for the Synthesis of Poly(Ethylene Oxide). *Biomacromolecules* **2017**, *18* (10), 3233−3237.

(18) Kamber, N. E.; Jeong, W.; Waymouth, R. M.; Pratt, R. C.; Lohmeijer, B. G. G.; Hedrick, J. L. Organocatalytic Ring-Opening Polymerization. *Chem. Rev.* **2007**, *107* (12), 5813−5840.

(19) Zhang, L.; Pratt, R. C.; Nederberg, F.; Horn, H. W.; Rice, J. E.; Waymouth, R. M.; Wade, C. G.; Hedrick, J. L. Acyclic Guanidines as

DOI: 10.1021/acs.macromol.9b01853
Macromolecules 2019, 52, 9238−9247

Organic Catalysts for Living Polymerization of Lactide. *Macromolecules* **2010**, *43* (3), 1660−1664.
(20) Chan, J. M. W.; Zhang, X.; Brennan, M. K.; Sardon, H.; Engler, A. C.; Fox, C. H.; Frank, C. W.; Waymouth, R. M.; Hedrick, J. L. Organocatalytic Ring-Opening Polymerization of Trimethylene Carbonate To Yield a Biodegradable Polycarbonate. *J. Chem. Educ.* **2015**, *92* (4), 708−713.
(21) Mezzasalma, L.; Dove, A. P.; Coulembier, O. Organocatalytic Ring-Opening Polymerization of L-Lactide in Bulk: A Long Standing Challenge. *Eur. Polym. J.* **2017**, *95*, 628−634.
(22) Pothupitiya, J. U.; Dharmaratne, N. U.; Jouaneh, T. M. M.; Fastnacht, K. V.; Coderre, D. N.; Kiesewetter, M. K. H-Bonding Organocatalysts for the Living, Solvent-Free Ring-Opening Polymerization of Lactones: Toward an All-Lactones, All-Conditions Approach. *Macromolecules* **2017**, *50* (22), 8948−8954.
(23) Xu, J.; Liu, J.; Li, Z.; Wang, H.; Xu, S.; Guo, T.; Zhu, H.; Wei, F.; Zhu, Y.; Guo, K. Guanidinium as Bifunctional Organocatalyst for Ring-Opening Polymerizations. *Polymer* **2018**, *154*, 17−26.
(24) Saito, T.; Aizawa, Y.; Tajima, K.; Isono, T.; Satoh, T. Organophosphate-Catalyzed Bulk Ring-Opening Polymerization as an Environmentally Benign Route Leading to Block Copolyesters, End-Functionalized Polyesters, and Polyester-Based Polyurethane. *Polym. Chem.* **2015**, *6* (24), 4374−4384.
(25) Bourissou, D.; Martin-Vaca, B.; Dumitrescu, A.; Graullier, M.; Lacombe, F. Controlled Cationic Polymerization of Lactide. *Macromolecules* **2005**, *38* (24), 9993−9998.
(26) Bednarek, M.; Basko, M.; Biedron, T.; Wojtczak, E.; Michalski, A. Polymerization of Lactide Initiated by Primary Amines and Catalyzed by a Protic Acid. *Eur. Polym. J.* **2015**, *71*, 380−388.
(27) Makiguchi, K.; Satoh, T.; Kakuchi, T. Diphenyl Phosphate as an Efficient Cationic Organocatalyst for Controlled/Living Ring-Opening Polymerization of δ-Valerolactone and ε-Caprolactone. *Macromolecules* **2011**, *44* (7), 1999−2005.
(28) Zhou, X.; Hong, L. Controlled Ring-Opening Polymerization of Cyclic Esters with Phosphoric Acid as Catalysts. *Colloid Polym. Sci.* **2013**, *291* (9), 2155−2162.
(29) Ren, Y.; Wei, Z.; Leng, X.; Wang, Y.; Li, Y. Boric Acid as Biocatalyst for Living Ring-Opening Polymerization of ε -Caprolactone. *Polymer* **2015**, *78*, 51−58.
(30) Persson, P. V.; Casas, J.; Iversen, T.; Córdova, A. Direct Organocatalytic Chemoselective Synthesis of a Dendrimer-like Star Polyester. *Macromolecules* **2006**, *39* (8), 2819−2822.
(31) Xu, J.; Song, J.; Pispas, S.; Zhang, G. Controlled/Living Ring-Opening Polymerization of ε -Caprolactone with Salicylic Acid as the Organocatalyst. *J. Polym. Sci., Part A: Polym. Chem.* **2014**, *52* (8), 1185−1192.
(32) Alamri, H.; Zhao, J.; Pahovnik, D.; Hadjichristidis, N. Phosphazene-Catalyzed Ring-Opening Polymerization of ε-Caprolactone: Influence of Solvents and Initiators. *Polym. Chem.* **2014**, *5* (18), 5471−5478.
(33) Wang, Y.; Niu, J.; Jiang, L.; Niu, Y.; Zhang, L. Benzo-12-Crown-4 Modified N -Heterocyclic Carbene for Organocatalyst: Synthesis, Characterization and Degradation of Block Copolymers of ε-Caprolactone with *L* -Lactide. *J. Macromol. Sci., Part A: Pure Appl. Chem.* **2016**, *53* (6), 374−381.
(34) Lohmeijer, B. G. G.; Pratt, R. C.; Leibfarth, F.; Logan, J. W.; Long, D. A.; Dove, A. P.; Nederberg, F.; Choi, J.; Wade, C.; Waymouth, R. M.; et al. Guanidine and Amidine Organocatalysts for Ring-Opening Polymerization of Cyclic Esters. *Macromolecules* **2006**, *39* (25), 8574−8583.
(35) Baśko, M.; Kubisa, P. Cationic Copolymerization of ε-Caprolactone and L, L-Lactide by an Activated Monomer Mechanism. *J. Polym. Sci., Part A: Polym. Chem.* **2006**, *44* (24), 7071−7081.
(36) Baśko, M.; Kubisa, P. Polyester Oligodiols by Cationic AM Copolymerization of L, L-Lactide and ε-Caprolactone Initiated by Diols. *J. Polym. Sci., Part A: Polym. Chem.* **2007**, *45* (14), 3090−3097.
(37) Mezzasalma, L.; De Winter, J.; Taton, D.; Coulembier, O. Extending the Scope of Benign and Thermally Stable Organocatalysts: Application of Dibenzoylmethane for the Bulk Copolymerization of L-Lactide and ε-Caprolactone. *J. Polym. Sci., Part A: Polym. Chem.* **2018**, *56* (5), 475−479.
(38) Mezzasalma, L.; De Winter, J.; Taton, D.; Coulembier, O. Benzoic Acid-Organocatalyzed Ring-Opening (Co)Polymerization (ORO(c)P) of L-Lactide and ε-Caprolactone under Solvent-Free Conditions: From Simplicity to Recyclability. *Green Chem.* **2018**, *20* (23), 5385−5396.
(39) Fliedel, C.; Vila-Viçosa, D.; Calhorda, M. J.; Dagorne, S.; Avilés, T. Dinuclear Zinc−N-Heterocyclic Carbene Complexes for Either the Controlled Ring-Opening Polymerization of Lactide or the Controlled Degradation of Polylactide Under Mild Conditions. *ChemCatChem* **2014**, *6* (5), 1481.
(40) Sattayanon, C.; Sontising, W.; Jitonnom, J.; Meepowpan, P.; Punyodom, W.; Kungwan, N. Theoretical Study on the Mechanism and Kinetics of Ring-Opening Polymerization of Cyclic Esters Initiated by Tin(II) n-Butoxide. *Comput. Theor. Chem.* **2014**, *1044*, 29−35.
(41) Li, P.; Xi, Y.; Li, L.; Li, H.; Sun, W.-H.; Lei, M. A DFT Study on Ring-Opening Polymerization of ε-Caprolactone Initiated by Mg and Al Complexes. *Inorg. Chim. Acta* **2018**, *477*, 34−39.
(42) Kazarina, O. V.; Gourlaouen, C.; Karmazin, L.; Morozov, A. G.; Fedushkin, I. L.; Dagorne, S. Low Valent Al(II)−Al(II) Catalysts as Highly Active ε-Caprolactone Polymerization Catalysts: Indication of Metal Cooperativity through DFT Studies. *Dalton Trans.* **2018**, *47* (39), 13800−13808.
(43) Nifant'ev, I.; Shlyakhtin, A.; Kosarev, M.; Karchevsky, S.; Ivchenko, P. Mechanistic Insights of BHT-Mg-Catalyzed Ethylene Phosphate's Coordination Ring-Opening Polymerization: DFT Modeling and Experimental Data. *Polymers* **2018**, *10* (10), 1105.
(44) Chuma, A.; Horn, H. W.; Swope, W. C.; Pratt, R. C.; Zhang, L.; Lohmeijer, B. G. G.; Wade, C. G.; Waymouth, R. M.; Hedrick, J. L.; Rice, J. E. The Reaction Mechanism for the Organocatalytic Ring-Opening Polymerization of l-Lactide Using a Guanidine-Based Catalyst: Hydrogen-Bonded or Covalently Bound? *J. Am. Chem. Soc.* **2008**, *130* (21), 6749−6754.
(45) Delcroix, D.; Couffin, A.; Susperregui, N.; Navarro, C.; Maron, L.; Martin-Vaca, B.; Bourissou, D. Phosphoric and Phosphoramidic Acids as Bifunctional Catalysts for the Ring-Opening Polymerization of ε-Caprolactone: A Combined Experimental and Theoretical Study. *Polym. Chem.* **2011**, *2* (10), 2249−2256.
(46) Nifant'ev, I.; Shlyakhtin, A.; Bagrov, V.; Lozhkin, B.; Zakirova, G.; Ivchenko, P.; Legon'kova, O. Theoretical and Experimental Studies of 1,5,7-Triazabicyclo[4.4.0]Dec-5-Ene-Catalyzed Ring Opening/Ring Closure Reaction Mechanism for 5-, 6- and 7-Membered Cyclic Esters and Carbonates. *React. Kinet., Mech. Catal.* **2016**, *117* (2), 447−476.
(47) Gazeau-Bureau, S.; Delcroix, D.; Martín-Vaca, B.; Bourissou, D.; Navarro, C.; Magnet, S. Organo-Catalyzed ROP of ε-Caprolactone: Methanesulfonic Acid Competes with Trifluoromethanesulfonic Acid. *Macromolecules* **2008**, *41* (11), 3782−3784.
(48) Susperregui, N.; Delcroix, D.; Martin-Vaca, B.; Bourissou, D.; Maron, L. Ring-Opening Polymerization of ε-Caprolactone Catalyzed by Sulfonic Acids: Computational Evidence for Bifunctional Activation. *J. Org. Chem.* **2010**, *75* (19), 6581−6587.
(49) Coady, D. J.; Horn, H. W.; Jones, G. O.; Sardon, H.; Engler, A. C.; Waymouth, R. M.; Rice, J. E.; Yang, Y. Y.; Hedrick, J. L. Polymerizing Base Sensitive Cyclic Carbonates Using Acid Catalysis. *ACS Macro Lett.* **2013**, *2* (4), 306−312.
(50) Coady, D. J.; Fukushima, K.; Horn, H. W.; Rice, J. E.; Hedrick, J. L. Catalytic insights into acid/base conjugates: highly selective bifunctional catalysts for the ring-opening polymerization of lactide. *Chem. Commun.* **2011**, *47*, 3105−3107.
(51) Frisch, M. J.; Trucks, G.; Schlegel, H. B.; Scuseria, G. E.; Robb, M. A.; Cheeseman, J.; Scalmani, G.; Barone, V.; Mennucci, B.; Petersson, G. A.; et al. *Gaussian 16, Revision B.1.*; Gaussian Inc.: Wallingford, CT, 2016.

DOI: 10.1021/acs.macromol.9b01853
Macromolecules 2019, 52, 9238−9247

(52) Chai, J.-D.; Head-Gordon, M. Long-Range Corrected Hybrid Density Functionals with Damped Atom−Atom Dispersion Corrections. *Phys. Chem. Chem. Phys.* **2008**, *10* (44), 6615.
(53) Cossi, M.; Barone, V.; Cammi, R.; Tomasi, J. Ab Initio Study of Solvated Molecules: A New Implementation of the Polarizable Continuum Model. *Chem. Phys. Lett.* **1996**, *255* (4), 327−335.
(54) Cancès, E.; Mennucci, B.; Tomasi, J. A New Integral Equation Formalism for the Polarizable Continuum Model: Theoretical Background and Applications to Isotropic and Anisotropic Dielectrics. *J. Chem. Phys.* **1997**, *107* (8), 3032−3041.
(55) Barone, V.; Cossi, M.; Tomasi, J. A New Definition of Cavities for the Computation of Solvation Free Energies by the Polarizable Continuum Model. *J. Chem. Phys.* **1997**, *107* (8), 3210−3221.
(56) Barone, V.; Cossi, M.; Tomasi, J. Geometry Optimization of Molecular Structures in Solution by the Polarizable Continuum Model. *J. Comput. Chem.* **1998**, *19* (4), 404−417.
(57) Mezzasalma, L.; Harrisson, S.; Saba, S.; Loyer, P.; Coulembier, O.; Taton, D. Bulk Organocatalytic Synthetic Access to Statistical Copolyesters from L-Lactide and ε-Caprolactone Using Benzoic Acid. *Biomacromolecules* **2019**, *20* (5), 1965−1974.

DOI: 10.1021/acs.macromol.9b01853
Macromolecules 2019, 52, 9238−9247